J. Biochem. **140**, 75–85 (2006)
doi:10.1093/jb/mvj125

Experimental Verification of the Crucial Roles of Glu^{73} in the Catalytic Activity and Structural Stability of Goose Type Lysozyme

Shunsuke Kawamura*, Kohji Ohno, Mari Ohkuma, Yuki Chijiiwa and Takao Torikata
Department of Bioscience, School of Agriculture, Kyushu Tokai University, Aso, Kumamoto 869-1404

Received March 29, 2006; accepted May 17, 2006

The roles of Glu^{73}, which has been proposed to be a catalytic residue of goose type (G-type) lysozyme based on X-ray structural studies, were investigated by means of its replacement with Gln, Asp, and Ala using ostrich egg-white lysozyme (OEL) as a model. No remarkable differences in secondary structure or substrate binding ability were observed between the wild type and Glu^{73}-mutated proteins, as evaluated by circular dichroism (CD) spectroscopy and chitin-coated celite chromatography. Substitution of Glu^{73} with Gln or Ala abolished the enzymatic activity toward both the bacterial cell substrate and *N*-acetylglucosamine pentamer, $(GlcNAc)_5$, while substitution with Asp did not abolish but drastically reduced the activity of OEL. These results demonstrate that the carboxyl group of Glu^{73} is directly involved in the catalytic action of G-type lysozyme. Furthermore, the stabilities of all three mutants, which were determined from the thermal and guanidine hydrochloride (GdnHCl) unfolding curves, respectively, were significantly decreased relative to those of the wild type. The results obtained clearly indicate the crucially important roles of Glu^{73} in the structural stability as well as in the catalytic activity of G-type lysozyme.

Key words: catalysis, goose type lysozyme, ostrich, site-directed mutagenesis, structural stability.

Abbreviations: G-type, goose type; C-type, chicken type; T4-type, phage type; OEL, ostrich egg-white lysozyme; GEL, goose egg-white lysozyme; HEL, hen egg-white lysozyme; T4L, T4 phage lysozyme; GlcNAc, *N*-acetylglucosamine; $(GlcNAc)_n$, β-1,4-linked oligosaccharide of GlcNAc with a polymerization degree of *n*; CD, circular dichroism; GdnHCl, guanidine hydrochloride; RP-HPLC, reverse-phase HPLC.

Lysozyme, one of the best characterized carbohydrolases, cleaves the glycosidic linkage between *N*-acetylglucosamine (GlcNAc) and *N*-acetylmuramic acid in bacterial cell walls. This enzyme is classified into three types, chicken type (C-type) (*1*–*3*), phage type (T4-type) (*4*, *5*), and goose type (G-type) (*6*–*8*), based on amino acid sequence similarity. These three different classes of lysozymes exhibit overall similarities in tertiary structure (*7*, *9*), although their amino acid sequences are almost entirely different. Much information on the structural properties and enzymatic mechanisms of C-type and T4-type lysozymes has been accumulated thus far. In particular, hen egg-white lysozyme (HEL) and T4 phage lysozyme (T4L) have been studied as model proteins for elucidating enzymatic function and protein stability. In contrast to C-type and T4-type lysozymes, however, information on G-type lysozyme is quite limited. The primary structure has been reported for only five G-type lysozymes, *i.e.*, those from ostrich (*10*), black swan (*11*), Embden goose (*6*), cassowary (*12*), and rhea (*13*), and three from the genes of chicken (*14*), flounder (*15*), and orange-spotted grouper (*16*). G-type lysozyme differs from the C-type in that it is much more specific for peptide-substituted substrate (*17*). C-type lysozyme hydrolyzes a homopolymer (chitin) effectively, while G-type lysozyme is a poor catalyst of the hydrolysis of this substrate. The differences in substrate specificity between these lysozymes are not well understood. Previously, Honda and Fukamizo reported the mode of binding of GlcNAc oligomer to goose egg-white lysozyme (GEL), and postulated that GEL has six substrate binding subsites (B-G sites) (*18*). This subsite structure was partly visualized in terms of the crystal structure of the GEL-$(GlcNAc)_3$ complex (*9*); however, part of the subsite structure (E-G sites) remains unknown.

The catalytic mechanism of HEL is considered to involve either an oxocarbonium ion intermediate (*19*–*22*) or a covalent enzyme-substrate intermediate (*23*), while that of T4L was found to be a single displacement mechanism (*24*, *25*). However, the mechanistic details of the catalytic reaction of G-type lysozyme remain unclear. The crystal structures of GEL, free and complexed with $(GlcNAc)_3$, revealed that the three-dimensional position of Glu^{73} in GEL is analogous to those of Glu^{35} in HEL and Glu^{11} in T4L, which are believed to act as a general acid to donate a proton to the glycosidic bond, thereby facilitating bond cleavage (*7*, *9*). It has therefore been proposed that Glu^{73} is a probable catalytic residue in G-type lysozyme. On the other hand, the X-ray structure of the GEL-$(GlcNAc)_3$ complex suggested that G-type lysozyme lacks a catalytic Asp residue that is a counterpart to either Asp^{52} in HEL, which is considered to stabilize the reaction intermediate, or Asp^{20} in T4L, which is thought to act as a base prompting a nucleophilic attack by water on the anomeric carbon (*9*). Glu^{35} in HEL and Glu^{11} in T4L have been shown to be

To whom correspondence should be addressed. Tel: +81-967-67-3918, Fax: +81-967-67-3960, E-mail: skawa@ktmail.ktokai-u.ac.jp

essential for the catalytic activity by means of chemical modifications and mutational analysis (*25–29*). However, hitherto no studies on the chemical modification and site-directed mutagenesis of G-type lysozyme have been carried out; thus, there has been no direct experimental evidence for the involvement of Glu^{73} in the catalytic action of G-type lysozyme. Although we can identify catalytic residues on X-ray analysis of an enzyme-substrate complex, kinetic analyses with site-specifically modified enzymes are required to confirm the identity or to determine the mechanism and degree of participation of these residues.

On the basis of sequence comparison of G-type lysozymes, we have shown that the amino acid sequences of three α-helices (α5, α7, and α8) are highly conserved in this enzyme group (*12*, *13*). These three α-helices are located at the center of the protein molecule and form a hydrophobic core in the overall structure of G-type lysozyme. In the crystal structure of GEL, the side chain of Glu^{73} on α5 (Ala^{64}–Glu^{73}) forms a hydrogen bond (2.68 Å) with the phenolic hydroxyl group of Tyr^{169} on α8 (Tyr^{169}–Gln^{182}) (Fig. 1). Since these two amino acids are completely conserved in G-type lysozyme (*13*), it was expected that Glu^{73}, in addition to its involvement as a critical catalytic residue, may also be important by maintaining the structural stability of G-type lysozyme through the interhelical hydrogen bond with Tyr^{169}. Therefore, we considered that a detailed study of Glu^{73} may provide a general insight for a better understanding of the structure–function relationship of G-type lysozyme.

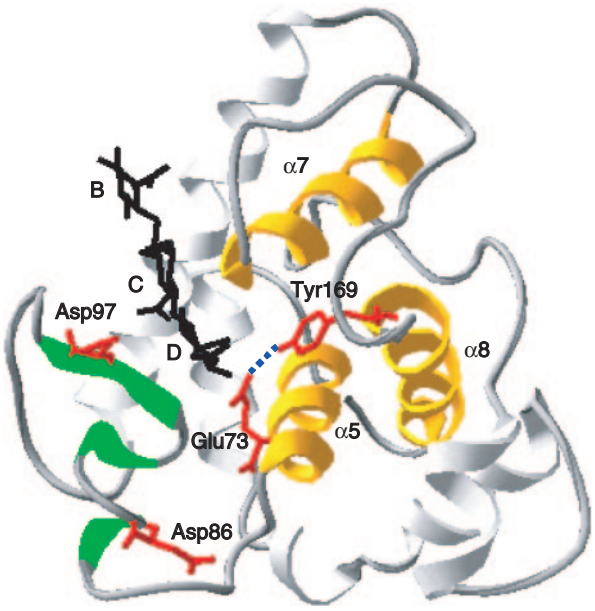

Fig. 1. **The three-dimensional structure of GEL complexed with $(GlcNAc)_3$.** The structure was created using the coordinate file PDB entry 154L (*9*). The side chains of amino acids (Glu^{73}, Asp^{86}, Asp^{97}, and Tyr^{169}) are shown in red. The three α-helices (α5, α7, and α8) and three β-sheets are shown in yellow and green, respectively. The hydrogen bond between Glu^{73} and Tyr^{169} is indicated by a dashed line. The three substrate binding subsites are represented by B, C, and D. The figure was generated using Swiss-PdbViewer (v3. 7b2).

Recently, we chemically synthesized the ostrich egg-white lysozyme (OEL) gene on the basis of the amino acid sequence and produced it in the yeast *Pichia pastoris* expression system, using the expression plasmid pPIC9K (*30*). This was the first report of a functional expression system for G-type lysozyme. However, the protein secreted by the transformed yeast was found to be processed at three different sites due to incorrect processing of the α-factor signal sequence. As a result, the yield of the purified OEL with the correct mature sequence was relatively low: about 10 mg/liter induced culture. For this reason, we first attempted in this study to synthesize a modified form of the OEL gene encoding an extra Ser at the N-terminus and to express it in the yeast expression system with the expectation that the correctly processed product before the introduced Ser residue could be obtained abundantly (hereinafter the resulting gene product is designated as the wild type). Next, we introduced mutations at position 73 into the modified gene and assessed the effects of the mutations on the catalytic activity and stability of OEL. We show that Glu^{73} is crucially important not only for the catalytic activity but also for the structural stability of G-type lysozyme.

MATERIALS AND METHODS

Materials—Restriction endonucleases and DNA-modifying enzymes were purchased from TaKaRa or Toyobo. The oligonucleotides used in this study were from Hokkaido System Science. *E. coli* strain JM109 was used for the transformation and propagation of recombinant plasmids. Plasmid pGEM-T was from Promega. Multi-Copy Pichia Expression kits, including the expression plasmid pPIC9K and host strain GS115, were obtained from Invitrogen. CM-Toyopearl 650M and *Micrococcus luteus* cells were from Tosoh and Sigma, respectively. *N*-Acetylglucosamine oligosaccharides [$(GlcNAc)_n$] were prepared by acid hydrolysis of chitin followed by charcoal celite column chromatography (*31*). Chitin-coated celite, an affinity adsorbent for lysozyme, was prepared by the method of Yamada *et al.* (*32*). Other reagents were of analytical or biochemical grade.

Preparation and Purification of the Wild Type with an Extra N-Terminal Ser Residue—The addition of an extra Ser residue to the N-terminus of OEL was performed by PCR from the synthesized OEL gene, using two oligonucleotide primers, 5′-GGCCTCGAGAAAAGATCTAGAACT-3′ and 5′-AAAAGCGGCCGCGAATTCTTATCAGTATCCA-TGTTGCTTG-3′ as sense and antisense primers, respectively. *Xho*I and *Eco*RI sites were introduced at the 5′- and 3′-ends of the amplified gene, respectively. The PCR product was subcloned into the pGEM-T vector, the resulting plasmid being designated as pGSer-OEL. The structure of the gene was confirmed by DNA sequence determination with an ABI PRIME 373A DNA Sequencer (Perkin-Elmer Applied Biosystems). Cloning to expression vector pPIC9K, transformation into *P. pastoris*, and overexpression were performed by the same procedures as those described in our previous paper (*30*). The wild type protein was purified as previously described, with slight modifications (*30*). The culture supernatant was diluted 4-fold with water and

then first put on a CM-Toyopearl column (4.0 × 12.5 cm) equilibrated with 30 mM sodium phosphate buffer (pH 7.0). After the column had been washed, the bound protein was eluted with 0.5 M NaCl in the same buffer. The eluate was diluted 4-fold with water and then loaded onto a CM-Toyopearl column (1.5 × 90 cm) equilibrated with 30 mM sodium phosphate buffer (pH 7.0). A linear gradient of NaCl, from 0.1 to 0.35 M, in the buffer was used for elution. The purified protein was dialyzed against distilled water and then lyophilized for storage. Its purity was confirmed by SDS-PAGE and reverse-phase HPLC (RP-HPLC) on a YMC-Pack C4 column (4.6 × 250 mm). The N-terminal amino acid sequence was determined with an Applied Biosystems model 477A sequencer. The protein concentration was measured by amino acid analysis with a Hitachi Model L-8500A amino acid analyzer.

Site-Directed Mutagenesis—The megaprimer method for site-directed mutagenesis (*33*) was used to introduce mutations at position 73, pGSer-OEL serving as a template. The mutagenic primers used were 5′-AGCATGAGATTGTCTAGAGAT-3′ for E73Q, 5′-AGCATGAGAATCTCTAGAGAT-3′ for E73D, and 5′-AGCATGAGAAGCTCTAGAGAT-3′ for E73A. After mutagenesis, all mutated genes were sequenced in their entirety to ensure that no alterations other than those expected had occurred. The mutant fragment was then recovered and ligated to the expression vector pPIC9K. Expression and purification of all mutants were performed in the same way as for the wild type.

CD Spectra—CD spectra were obtained at 25°C with a Jasco J-600 spectropolarimeter. Proteins were dissolved to a final concentration of 0.15 mg/ml in 10 mM sodium acetate buffer (pH 5.0). The data are expressed in terms of mean residue ellipticity. The path-length of the cells was 0.1 cm for far-ultraviolet CD spectra (200–250 nm).

Substrate Binding—The binding of the wild type and mutant proteins to GlcNAc polymer, *i.e.*, chitin, was examined by affinity chromatography on a chitin-coated celite column (0.75 × 7.5 cm). Proteins (0.16 mg) were first eluted with a gradient from 20 ml of 10 mM sodium phosphate buffer (pH 7.0) to 20 ml of the same buffer containing 1 M NaCl, and then eluted with 1 M NaCl in the buffer isocratically at a flow rate of 0.5 ml/min. The chromatography was performed at 0°C by dipping the column in an ice-water bath. Protein elution was monitored as the absorbance at 280 nm.

Assaying of Enzymatic Activity—Bacteriolytic activity (lytic activity) of lysozyme was assayed using lyophilized cells of *M. luteus* as a substrate. One hundred microliters of lysozyme (final concentration to be 0.015 μM) was added to 3 ml of a suspension of *M. luteus* adjusted to OD 1.0 at 540 nm with 0.1 M sodium phosphate buffer (pH 7.0). The enzyme-catalyzed decrease in OD_{540} was followed at 25°C for 30 min. The decrease in OD_{540} caused by H_2O (100 μl) under the same conditions was also measured as a control.

Lysozyme-catalyzed hydrolysis of $(GlcNAc)_5$ was analyzed using a TSK Amide 80 column (4.6 × 250 mm; Tosoh) in a JASCO 800 series HPLC (*30*).

Thermal Unfolding—Thermal unfolding curves were determined by monitoring the CD value at 222 nm with a Jasco J-600 spectropolarimeter using a 0.1-cm cuvette. Samples with a concentration of 0.15 mg/ml were dissolved in 0.1 M sodium acetate buffer (pH 5.0) containing 0.5 M guanidine hydrochloride (GdnHCl). The water-jacketed cell containing each sample was heated for 5 min at a given temperature by a thermostatically regulated circulating water bath. All samples were fully equilibrated at each temperature before measurement. The temperature of sample solutions was directly measured using a thermometer, TX1001 (Yokokawa M&C Co.). Thermal unfolding curves were also obtained under the same conditions, except for the protein concentration (0.015 mg/ml), by monitoring the decrease in the intrinsic fluorescence emission at 360 nm with excitation at 280 nm. Fluorescence measurements were performed with a Hitachi F-4500 Fluorescence Spectrophotometer using a 1-cm cuvette. The reversibility of the unfolding transition was estimated by comparison of either the CD value or fluorescence intensity obtained after annealing with that obtained before raising of the temperature, and was more than 95% for all proteins tested. To facilitate comparison between the two sets of unfolding curves, the experimental data were normalized as follows. The fraction of unfolded protein was calculated from either the CD values or fluorescence intensities by linearly extrapolating the pre- and post-transition base lines to the transition zone, and then plotted against temperature. Assuming that the unfolding equilibrium involves a two-state mechanism, the unfolding curves were subjected to least squares analysis to determine the midpoint temperatures (T_m) and thermodynamic parameters. The enthalpy and entropy changes at T_m (ΔH_m and ΔS_m) were calculated using van't Hoff analysis. The difference in the free energy change of unfolding (at T_m of the wild type protein) between the mutant and wild type proteins ($\Delta\Delta G$) was estimated by the relationship, $\Delta\Delta G = \Delta T_m \cdot \Delta S_m$ (wild type), given by Becktel and Schellman (*34*), where ΔT_m is the difference in T_m between the mutant and wild type proteins and ΔS_m (wild type) is the entropy change of the wild type protein at T_m.

GdnHCl Unfolding—GdnHCl-induced unfolding curves were also determined by monitoring two different parameters at 30°C. One is the CD value at 222 nm and the other is the intrinsic fluorescence (excitation at 280 nm and emission at 360 nm). The protein concentrations were 0.15 mg/ml for CD and 0.015 mg/ml for fluorescence, respectively. Samples were incubated in 0.1 M sodium acetate buffer (pH 5.0) with varying concentrations of GdnHCl at 30°C for 1 h. All samples were fully equilibrated at each denaturant concentration before measurement. Denaturation was completely reversible under these conditions and the unfolding data were analyzed based on a two-state model. From the GdnHCl unfolding profiles, the difference in free energy change between the folded and unfolded states (ΔG) was calculated according to Pace (*35*). The free energy change in water (ΔG^{H_2O}) and the dependence of ΔG on the GdnHCl concentration (m) were determined by least-squares fitting of the data for the transition region using the equation $\Delta G = \Delta G^{H_2O} - m[\text{GdnHCl}]$. The GdnHCl concentration at the midpoint of the transition ($\Delta G = 0$) was defined as C_m. The differences in C_m (ΔC_m) between the wild type and mutant proteins were calculated by subtracting the value for the wild type from those of mutant proteins.

RESULTS

Production and Characterization of the Wild Type with an Extra N-Terminal Ser Residue—We recently constructed an expression plasmid for OEL, which exhibits 84% amino acid identity with GEL, as a downstream fusion to the α-factor signal sequence gene preceded by the alcohol oxidase gene *AOX1* promoter, the objective being secretion of recombinant OEL into the growth medium (*30*). However, in addition to the mature OEL, misprocessed OEL molecules with three or four additional amino acids of the α-factor signal sequence attached to the N-terminus were also produced in this system. Misprocessed sub-products have also been found when other C-type lysozymes with an N-terminal Lys residue are expressed in a yeast expression system using α-factor as a secretion signal (*36–38*). We speculated that the bulky side chain of Arg^{1}, which is the N-terminal amino acid residue of OEL, might be relevant to the observed incorrect processing of the signal sequence. Since it was previously reported that the characteristics of HEL with an extra Ser residue added to its N-terminus were almost identical with those of the authentic protein (*39*, *40*), we attempted to insert a Ser residue between the C-terminus of the α-factor signal and the N-terminus of OEL in order to prevent the incorrect processing.

The recombinant protein secreted into the medium was purified as described under "MATERIALS AND METHODS." The purified protein was found to be homogeneous on analysis by SDS-PAGE and gave a single peak on RP-HPLC (data not shown). As expected, direct N-terminal sequencing provided a single sequence: Ser-Arg-Thr-Gly. This result indicated specific cleavage at the C-terminus of the α-factor signal, giving rise to OEL with an extraneous Ser residue at the N-terminus. The purified wild type protein was found to possess enzymatic properties similar to those of authentic OEL in terms of the far-UV CD spectrum (Fig. 2), substrate binding ability (Fig. 3), lytic activity (Fig. 4), and structural stability (Fig. 6 and Tables 1 and 2). The yield of the wild type was ~80 mg/liter culture, which was about eight times more than that obtained with our previous method (*30*). Therefore, the addition of an extra Ser residue to the N-terminus of OEL was considered to be useful for the preparation of large amounts of mutant proteins.

Expression and Characterization of Mutant Proteins—Based on the crystal structures of GEL, free and complexed with $(GlcNAc)_3$, Glu^{73} in G-type lysozyme has previously been proposed to be a probable catalytic residue analogous to Glu^{35} in HEL and Glu^{11} in T4L (*7*, *9*). However, no experimental evidence showing that the carboxyl group of Glu^{73} is directly involved in the catalytic action of G-type lysozyme has been reported thus far. Therefore, to demonstrate the involvement of Glu^{73} as a critical catalytic residue of G-type lysozyme, three mutant proteins (E73Q, E73D, and E73A) were constructed by site-directed mutagenesis. All mutants were purified to homogeneity, and their purity was evaluated by SDS-PAGE and RP-HPLC (data not shown). The yields of the mutant proteins were comparable to that of the wild type, *i.e.*, approximately 60 mg/liter. The N-terminal amino acid sequences of the mutants were identical to that of the wild type, indicating that each mutant has an extra Ser residue at the N-terminus. Far-UV CD spectra of the mutants were essentially the same as that of the wild type (Fig. 2), indicating that these mutations caused no structural perturbations.

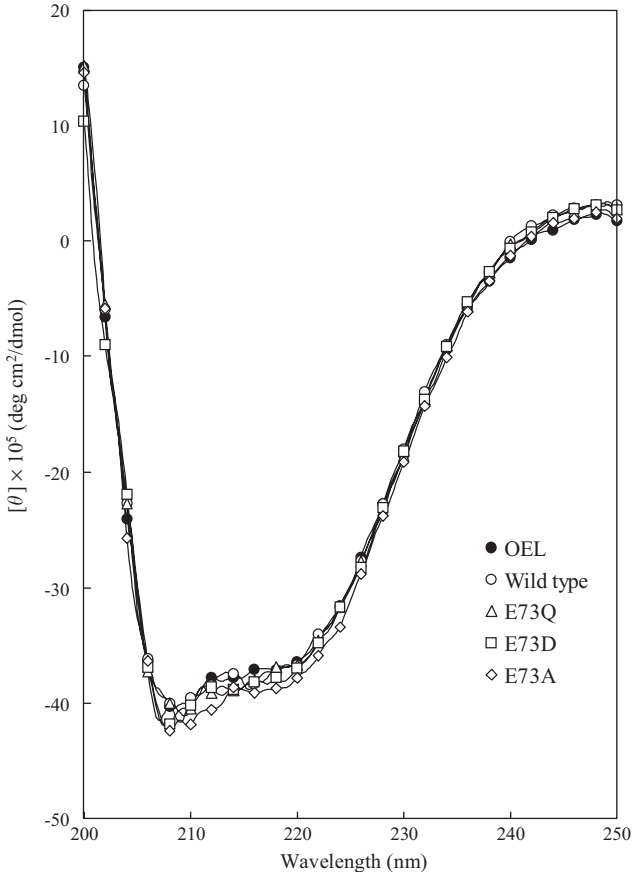

Fig. 2. **CD spectra of authentic OEL, the wild type, and Glu^{73}-mutated proteins in the far-ultraviolet region.**

Effects of Mutations on Substrate Binding Ability—Oligosaccharide binding experiments on carbohydrolases have been performed using physicochemical methods, such as fluorescence, CD, and NMR spectroscopy (*41–44*). In particular, tryptophan fluorescence observation is useful for a binding study because of its high sensitivity. However, a suitable localization of the tryptophan residues in the protein molecule is required to observe a change in the fluorescence spectrum upon saccharide binding. In our preliminary experiments, we failed to observe a change in the fluorescence spectrum of OEL upon the oligosaccharide addition. On the other hand, chitin-coated celite has been used as an affinity adsorbent for HEL and its mutants to examine the substrate binding abilities of the whole saccharide binding sites (A–F sites) (*45–48*). Thus, we applied this method to evaluate the substrate binding abilities (through B–G sites) of the wild type and mutant proteins by comparing the relative elution positions on a chitin-coated celite column (Fig. 3). When BSA was used as a control, it was completely excluded from the affinity column (Fig. 3C). As for E73Q and E73D, they were adsorbed on the column and were eluted as a single peak at almost the same positions as that of the wild

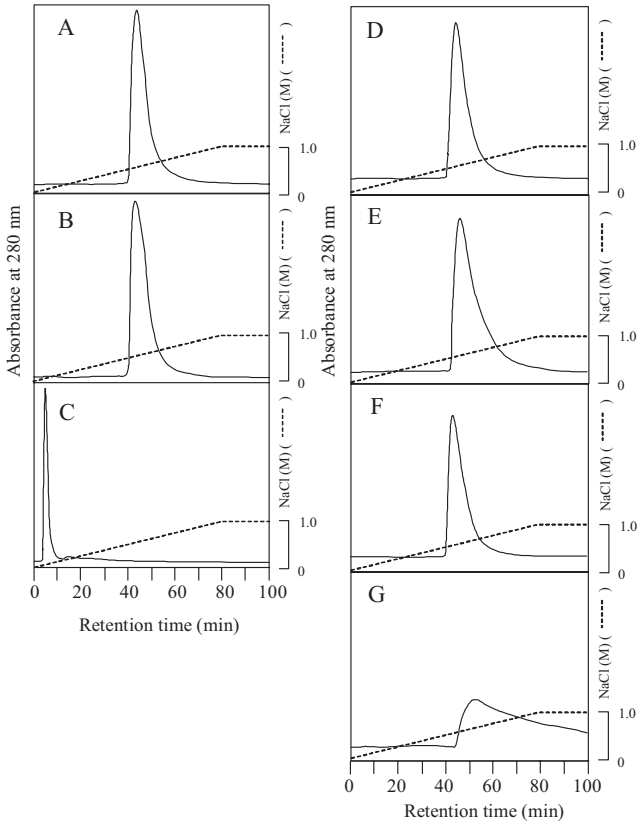

Fig. 3. **HPLC of authentic OEL, the wild type, and Glu[73]-mutated proteins on a chitin-coated celite column (0.75 × 7.5 cm).** BSA was used as a control. (A) authentic OEL; (B) wild type; (C) BSA; (D) wild type; (E) E73Q; (F) E73D; (G) E73A.

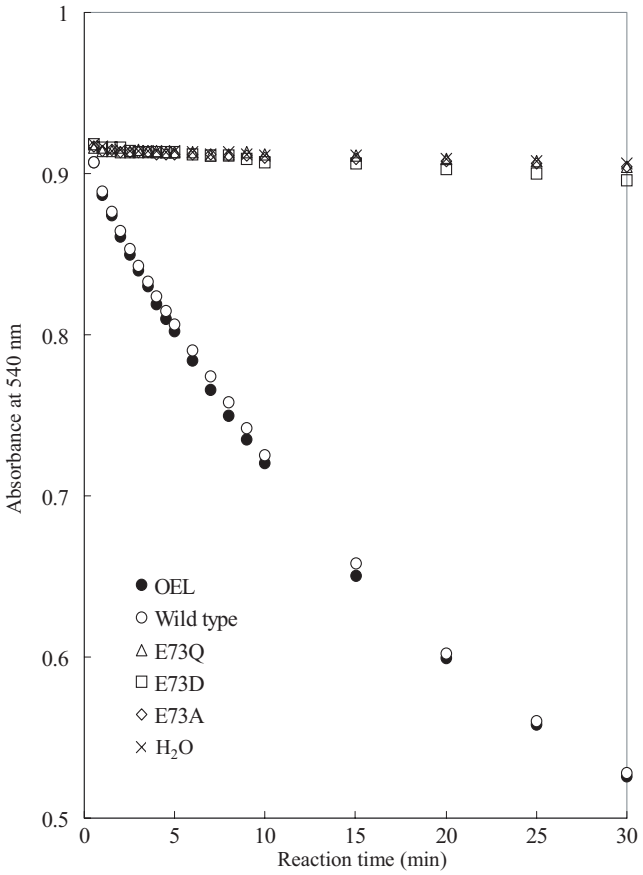

Fig. 4. **Lysis of *M. luteus* by authentic OEL, the wild type, and Glu[73]-mutated proteins.** The enzyme-catalyzed decrease in OD_{540} was followed at 25°C for 30 min. The decrease in OD_{540} caused by H_2O under the same conditions was also measured as a control.

type with a linear gradient of 0 to 1 M NaCl. The elution profile of E73A totally changed to a broad peak, which continued to be eluted gradually over 1 M NaCl. The elution position of E73A was a little later than those of the wild type and other mutants, suggesting a higher affinity of E73A for chitin than the other proteins. As an explanation for this phenomenon, the substrate binding ability of E73A might be enhanced by an increase in the hydrophobicity of the replaced Ala[73]. Anyway, the results obtained suggest that the substrate binding ability is well conserved by the mutant proteins.

Effects of Mutations on Catalytic Activity—Preliminary evaluation of enzyme activity was performed by monitoring the enzyme-catalyzed lysis of *M. luteus* cells, which is a high-molecular-weight polymeric substrate with a highly negative charge (Fig. 4). Substitution of the Glu[73] residue severely impaired the lytic activity. Replacing Glu[73] with Gln or Ala decreased the catalytic activity of the enzyme to a nearly undetectable level, and the lysis profiles of these mutants were almost the same as that seen in the control experiment. Similar results were also obtained using the increased concentration (0.15 μM) of the two mutants in the assay solution (data not shown). On the other hand, E73D was found to exhibit a detectable level of activity, but its activity was drastically reduced as compared with the lysis curve of the wild type, suggesting the possible involvement of the carboxyl group of Asp[73] in the catalytic action. These results suggest an essential role of the carboxyl group of Glu[73] in catalysis.

Since the substrate used for lytic activity is chemically heterogeneous, the catalytic activity of the Glu[73] mutants was more precisely evaluated by measuring the enzyme-catalyzed hydrolysis of $(GlcNAc)_5$ with a well-defined uniform chemical structure (Fig. 5). The wild type protein hydrolyzed the initial substrate $(GlcNAc)_5$ almost completely on 140 min reaction, and $(GlcNAc)_5$ was hydrolyzed mainly to $(GlcNAc)_2$ + $(GlcNAc)_3$ with much less cleavage into $(GlcNAc)_1$ + $(GlcNAc)_4$. Consistent with the results obtained in the *M. luteus* assay, no hydrolysis of $(GlcNAc)_5$ was observed for E73Q or E73A at 50°C for 48 h. Although E73D hydrolyzed $(GlcNAc)_5$ to produce $(GlcNAc)_2$ and $(GlcNAc)_3$ as in the case of the wild type, the overall reaction speed of E73D was extremely reduced as compared with that of the wild type: only small amounts of products were generated in 48 h in the E73D-catalyzed reaction.

The fact that E73Q and E73A were virtually inactive with little change in secondary structure and substrate binding ability indicates that the lack of activity results from the loss of an essential functional group of Glu[73]. Furthermore, the extremely low activity observed for E73D, in which the spatial position of carboxyl group of

Table 1. **Parameters characterizing the thermal denaturation of authentic OEL, the wild type, and the three mutants of it.** Thermodynamic parameters were calculated from the thermal unfolding curves presented in Figs. 6A and 7A. All values are the averages of at least two determinations.

Protein	Method	ΔH_m (kcal/mol)	ΔS_m (kcal/mol°K)	T_m (°C)	ΔT_m (°C)	$\Delta\Delta G$ (kcal/mol)
Wild type	Flu[a]	170.1	0.510	60.6		
OEL	Flu[a]	170.2	0.512	59.6	–1.0	–0.51
E73A	Flu[a]	156.7	0.475	57.4	–3.2	–1.63
E73Q	Flu[a]	151.2	0.459	56.6	–4.0	–2.04
E73D	Flu[a]	154.8	0.473	54.5	–6.1	–3.11
Wild type	CD	166.9	0.501	60.5		
E73D	CD	146.0	0.445	54.8	–5.7	–2.86

[a]Fluorescence.

Table 2. **Parameters characterizing the GdnHCl denaturation at pH 5.0 and 30°C.** Parameters were calculated from the GdnHCl unfolding curves presented in Figs. 6B and 7B. All values are the averages of at least two determinations.

Protein	Method	m (kcal/molºM)	C_m (M)	ΔC_m (M)	ΔG^{H_2O} (kcal/mol)	$\Delta\Delta G^{H_2O}$ (kcal/mol)
Wild type	Flu[a]	5.48	2.21		12.11	
OEL	Flu[a]	5.22	2.25	+0.04	11.77	–0.34
E73A	Flu[a]	5.78	1.89	–0.32	10.90	–1.21
E73Q	Flu[a]	5.98	1.75	–0.46	10.49	–1.62
E73D	Flu[a]	5.97	1.70	–0.51	10.17	–1.94
Wild type	CD	5.32	2.20		11.73	
E73D	CD	5.91	1.72	–0.48	10.15	–1.58

[a]Fluorescence.

the 73rd residue is changed, indicates that the relative disposition of the Glu^{73} carboxyl group as to a substrate is critical for catalytic activity. It is thus concluded that Glu^{73} is absolutely required for the catalytic activity of G-type lysozyme.

Effects of Mutations on Structural Stability—To evaluate the contribution of Glu^{73} to the structural stability of OEL, we initially analyzed thermal unfolding of the wild type and mutant proteins in 0.1 M sodium acetate buffer (pH 5.0). When the thermal denaturation curves were analyzed in the absence of GdnHCl, the reversibility calculated was 76% for the wild type, 80% for E73D, 80% for E73Q, and 79% for E73A. The T_m values obtained on fluorescence measurement were 67.3, 66.2, 63.9, and 62.2°C for the wild type, E73A, E73Q, and E73D, respectively, in the absence of GdnHCl (data not shown). On the other hand, in the presence of 0.5 M GdnHCl, the reversibility of the thermal unfolding for the wild type and mutant proteins was confirmed to be more than 95%, indicating that the unfolding transitions are essentially reversible under the conditions employed. Hence, we analyzed precisely the thermal denaturation of the wild type and mutant proteins in the presence of 0.5 M GdnHCl by both CD and fluorescence measurements. The thermal unfolding curves of the wild type, normalized as to the fraction of unfolded protein, are shown in Fig. 6A. The unfolding transition curves derived from the CD and fluorescence data were coincident with each other, indicating that the unfolding transition of the wild type is well represented by a two-state mechanism, in which only the native and unfolded states are present in the transition zones. This enabled us to determine the values of T_m and thermodynamic parameters for the unfolding process of the wild type (Table 1). The T_m value obtained on CD measurement for the wild type (60.5°C) showed good agreement with that determined on fluorescence measurement (60.6°C).

The thermal unfolding curves of the wild type and three mutant proteins obtained on fluorescence measurement are shown in Fig. 7A. All transitions were characterized by the presence of a single sharp change in the fluorescence intensity that is typical of cooperative transition in a two-state system. The mutations of Glu^{73} had significant effects on the thermal unfolding of the mutant proteins: the T_m values for E73A, E73Q, and E73D decreased by 3.2, 4.0, and 6.1°C, respectively, compared to 60.6°C for the wild type (Table 1). The Glu^{73} mutations reduced the thermostability of the proteins by 1.63, 2.04, and 3.11 kcal/mol for E73A, E73Q, and E73D, respectively, at 60.6°C. We also used CD to monitor the heat-induced unfolding of the most destabilized mutant, E73D (Fig. 6A). As in the case of the wild type, the thermal unfolding curve of E73D coincided well with that obtained from the fluorescence data and clearly showed the thermal destabilization of E73D as compared with the wild type: ΔT_m = –6.1°C for fluorescence and ΔT_m = –5.7°C for CD (Table 1).

The contribution of Glu^{73} to the structural stability of OEL was further assessed by means of unfolding experiments with GdnHCl as a denaturant (Figs. 6B and 7B). As expected from the thermal unfolding experiment, the GdnHCl-induced unfolding curves of the wild type derived from the CD and fluorescence data were coincident with each other (Fig. 6B), further confirming that the wild type protein is denatured with a two-state transition model. The thermodynamic parameters for denaturation induced with GdnHCl are listed in Table 2. The C_m and ΔG^{H_2O} values obtained with CD for the wild type were almost identical with those determined with fluorescence.

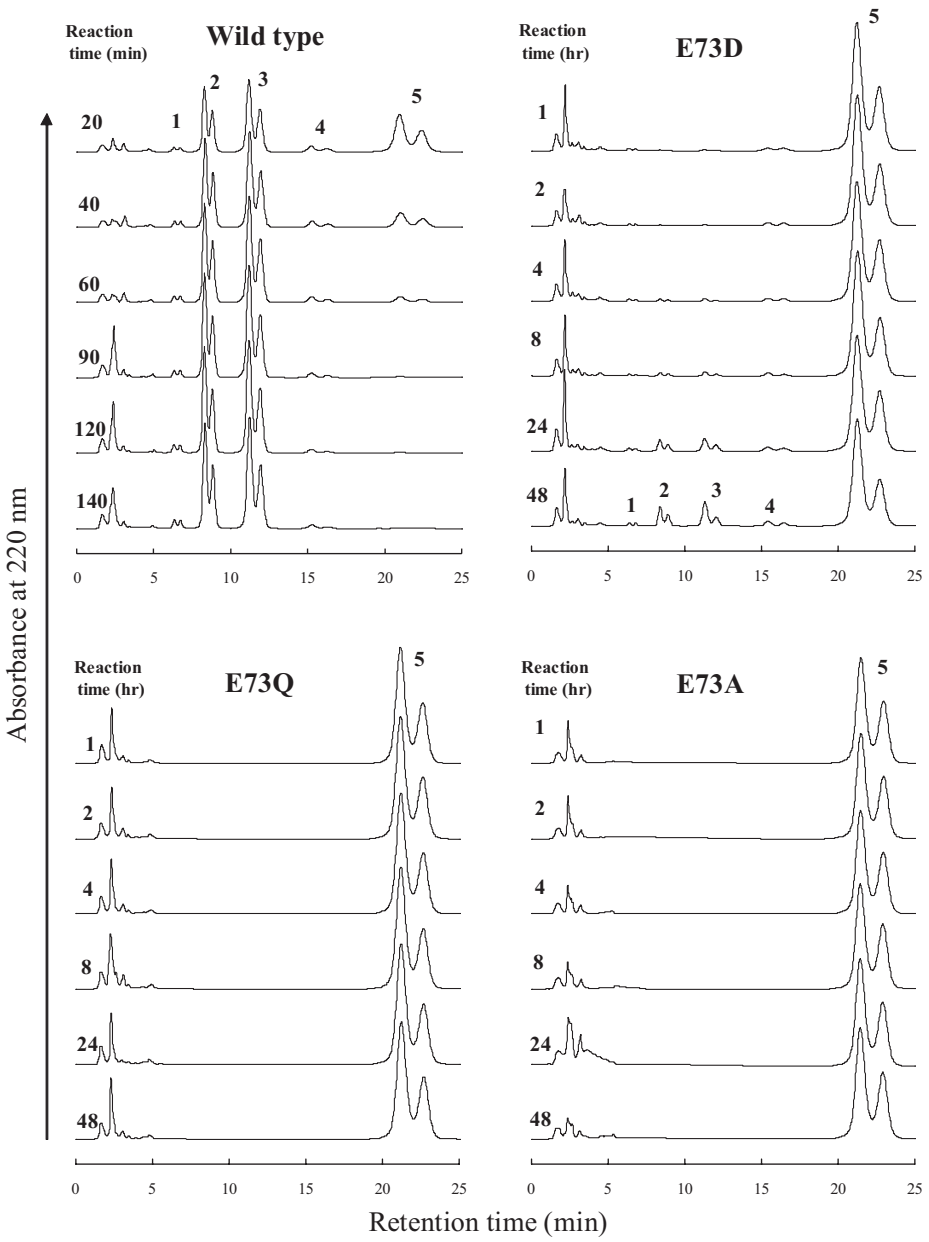

Fig. 5. **HPLC profiles showing the enzymatic hydrolysis of $(GlcNAc)_5$.** The enzymatic reaction was performed in 10 mM sodium acetate buffer (pH 4.0) at 50°C. Numerals in the figures are the polymerization degrees of the reaction product species.

Figure 7B shows the GdnHCl-induced unfolding curves of the wild type and mutant proteins obtained on fluorescence measurement. The transitions of the mutant proteins were highly cooperative. The unfolding transitions of all mutant proteins occurred at lower concentrations of GdnHCl than that of the wild type: the C_m values were reduced, as compared with that of the wild type, by 0.32, 0.46, and 0.51 M for E73A, E73Q, and E73D, respectively (Table 2). The ΔG^{H_2O} values of unfolding indicated that the three mutants, E73A, E73Q, and E73D, were destabilized by 1.21, 1.62, and 1.94 kcal/mol, respectively, at 0 M GdnHCl in comparison to the wild type. The stability of the least stable mutant, E73D, against GdnHCl was further analyzed by CD measurement (Fig. 6B). The coincidence of the two transition curves derived from the CD and fluorescence data was also observed for E73D: the ΔC_m and $\Delta\Delta G^{H_2O}$ values obtained with CD were –0.48 M and –1.58 kcal/mol, respectively, being in agreement with the data determined with fluorescence (Table 2). These findings further support the results obtained in the thermal unfolding experiments and confirm the importance of Glu[73] in the structural stability of G-type lysozyme.

DISCUSSION

This study provided direct experimental proof for the involvement of Glu[73] in the catalytic action of G-type lysozyme. It also showed that Glu[73] plays an important role in the structural stability of G-type lysozyme. Although the exact catalytic mechanism of G-type lysozyme remains unclear at this stage, Monzingo *et al.* have provided important information on the structural similarity among G-type lysozyme, T4L, barley chitinase

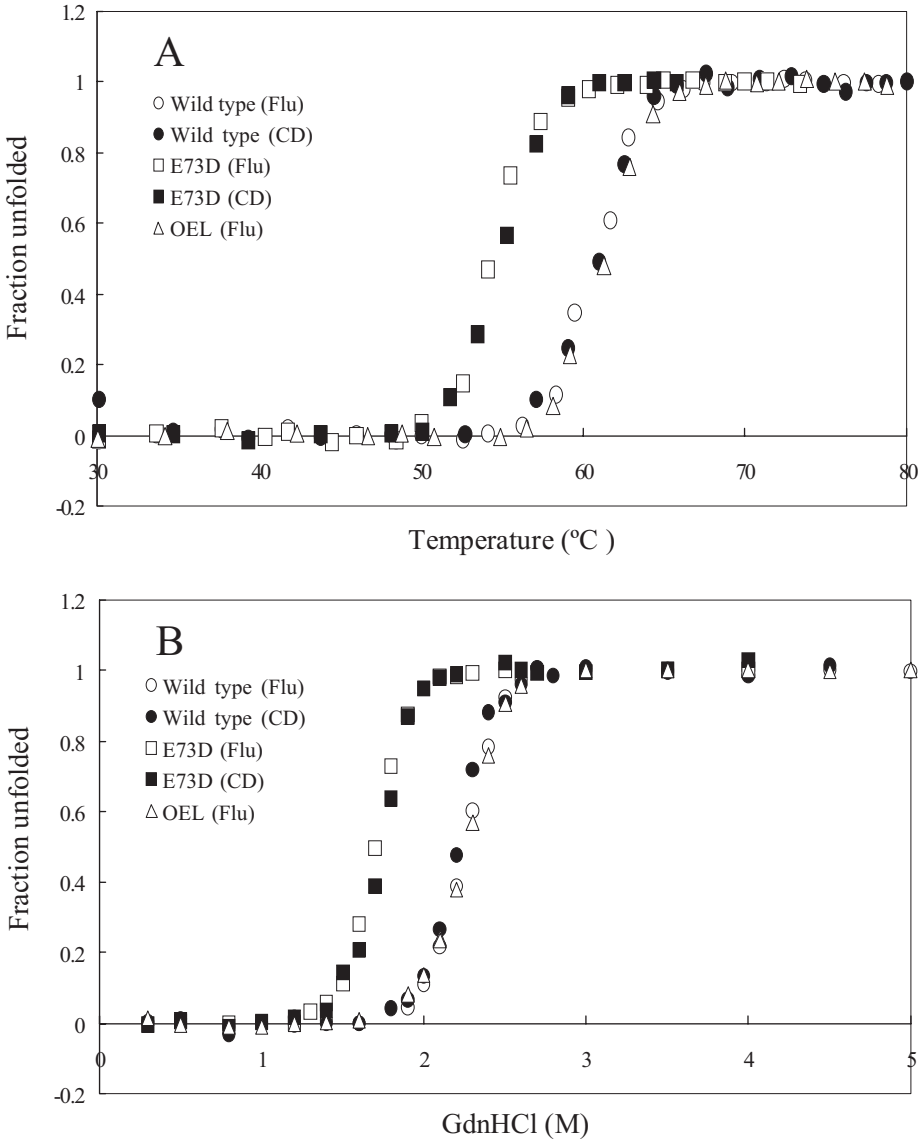

Fig. 6. **Thermal and GdnHCl-induced unfolding curves of authentic OEL, the wild type, and E73D obtained by CD and fluorescence measurements.** Panels A and B show the thermal and GdnHCl unfolding curves, respectively. The experimental details are given under "MATERIALS AND METHODS." The unfolding curves of the wild type and E73D obtained with CD are indicated as "Wild type (CD)" and "E73D (CD)," respectively, while those of authentic OEL, the wild type, and E73D obtained with fluorescence are indicated as "OEL (Flu)," "Wild type (Flu)," and "E73D (Flu)," respectively.

(family 19), and *Streptomyces* sp. N174 chitosanase (family 46), despite the differences in their amino acid sequences (*49*). Based on structural criteria, these enzymes were further divided into a prokaryotic family (*Streptomyces* sp. N174 chitosanase and T4L) and a eukaryotic family (barley chitinase and G-type lysozyme). The structural similarity between barley chitinase and G-type lysozyme implies that these two enzymes may exhibit similarity in the catalytic mechanism. It was previously reported that barley chitinase produces an α-anomer through hydrolysis of the β-1,4 glycosidic linkage (anomer inversion) (*50*, *51*), and the catalytic reaction is thought to involve the single displacement mechanism (*49*). The reactions of the structurally related *Streptomyces* sp. N174 chitosanase and T4L also proceed with inversion of the product anomer (*25*, *49*, *52*). According to the mechanism for inverting glycosyl hydrolases, one of the two catalytic (carboxylic acid) residues acts as a general acid and the other as a general base (*53*). The Glu^{73} residue probably acts as the general acid catalyst in G-type lysozyme in analogy with Glu^{11} in T4L, Glu^{67} in barley chitinase (*54*), and Glu^{22} in *Streptomyces* sp. N174 chitosanase (*55*). In addition to Glu^{73}, two amino acid residues with carboxyl groups (Asp^{86} and Asp^{97}), which are conserved in all known G-type lysozymes, are located in the active site of this enzyme group (Fig. 1). The crystal structure of GEL complexed with $(GlcNAc)_3$ bound at B–D sites has suggested that these two residues are not directly involved in the catalytic action of G-type lysozyme, because they are more than 5 Å from the C1 carbon of the site D sugar (*9*). From this information, a second acidic residue analogous to Asp^{20} in T4L, Glu^{89} in barley chitinase, and Asp^{40} in *Streptomyces* sp. N174 chitosanase is thought to be not required for the catalytic activity of G-type lysozyme. However, as illustrated by the analyses of Asn^{229} in thymidylate synthase (*56*, *57*), site-directed mutagenesis studies are required for a reliable elucidation of the functional importance of individual amino acids at the active site of a known structure (*58*). Therefore, the possibility of the involvement of Asp^{86} or Asp^{97} or both in the catalytic

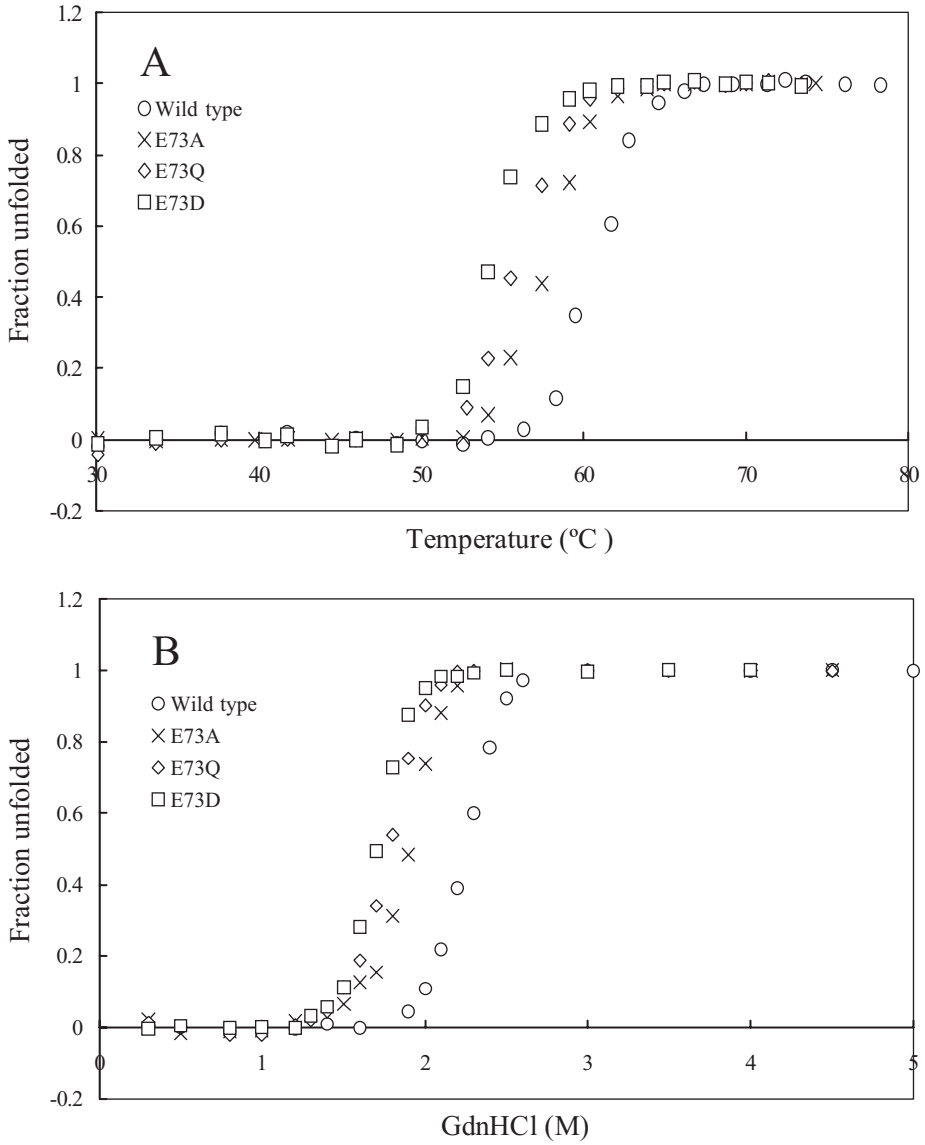

Fig. 7. **Thermal and GdnHCl-induced unfolding curves of the wild type, E73Q, E73D, and E73A obtained by fluorescence measurements.** Panels A and B show the thermal and GdnHCl unfolding curves of the wild type and Glu[73]-mutated proteins, respectively. The experimental details are given under "MATERIALS AND METHODS."

action of G-type lysozyme still cannot be ignored. Further functional studies are necessary to elucidate the details of the roles played by residues of unknown functional importance, such as Asp[86] and Asp[97], in the catalytic mechanism of G-type lysozyme.

The crystal structure of GEL shows that the Glu[73] side chain interacts with the Tyr[169] ring hydroxyl group through hydrogen bonding (Fig. 1). Glu[73] and Tyr[169] are located at the C-terminus of α5 and the N-terminus of α8, respectively. We have shown that G-type lysozyme has a structurally invariant core composed of three α-helices (α5, α7, and α8) (*12*, *13*). Since Glu[73] and Tyr[169] are completely conserved amino acids in G-type lysozymes (*13*), the Glu[73]–Tyr[169] interaction is thought to be a common structural feature in this enzyme group. It seems therefore likely that the interhelical hydrogen bond formed between these two residues is responsible for the stabilization of the hydrophobic core structure consisting of the three α-helices. Actually, the structural stability of the Glu[73] mutant is decreased relative to that of the wild type. In the case of E73D, the replacement of Glu[73] by Asp[73] with a shorter side chain is considered to remove or weaken the hydrogen bond with Tyr[169]. This is probably one of the main reasons why E73D is the least stable among the mutant proteins. As for E73Q, it was found to be more stable than E73D. Since the side chain of glutamine is almost equal in size to that of glutamic acid, it is suggested that the Glu[73]–Tyr[169] interaction may be partly compensated for by the rearrangement of a hydrogen bond formed between the carboxamide group of the substituted Gln[73] and the hydroxyl group of Tyr[169]. On the other hand, an unexpected result was obtained for the mutant E73A. Since the hydrogen bond with Tyr[169] is lost in E73A, the stability of this variant was expected to be almost identical to or lower than that of E73D. However, E73A was shown to be the most stable among the three mutant proteins. The decreased stabilities of E73D and E73Q relative to that of E73A may be ascribed to the introduced polar groups in place of the methyl group of the Ala[73] side chain in a hydrophobic environment.

The side chain conformational entropy might also contribute to the increase in the stability of E73A relative to those of other mutants. Although the three-dimensional structures of the Glu^{73} mutants are required to understand the mechanisms by which these mutant proteins are destabilized, our data indicate that the side chain of Glu^{73} is strongly involved in the structural stability of G-type lysozyme.

It was previously reported for T4L that residues in a protein that participate in catalysis are not optimal for stability (*59*). Six mutations at two catalytic residues (Glu^{11} and Asp^{20}) and nine mutations at two substrate binding residues (Ser^{117} and Asn^{132}) abolished or reduced the enzymatic activity but increased the thermal stability of T4L. Like the substitutions at Glu^{11} in T4L, two mutations at Glu^{35} (Glu^{35} to Gln and Ala) eliminated the activity but increased the stability of HEL (*46*). Similar results have been reported for other proteins (*60–62*). In the case of G-type lysozyme, however, the Glu^{73} mutations eliminated the catalytic activity and reduced the stability against thermal and GdnHCl denaturation. Therefore, the present study not only demonstrates the critical involvement of Glu^{73} in the catalytic activity but also indicate the additional crucial role of the Glu^{73} residue in the structural stability of G-type lysozyme.

We further consider that the hydrogen bonding interaction between Glu^{73} and Tyr^{169} may also serve to hold the carboxyl group of Glu^{73} in the proper orientation optimal for catalysis. In other words, Glu^{73} may not be able to play a catalytic role efficiently when not assisted by the hydrogen bond with Tyr^{169}. To address the importance of Tyr^{169} in assisting the enzyme catalysis of G-type lysozyme, site-directed mutagenesis studies on various Tyr^{169} mutants are in progress.

REFERENCES

1. Canfield, R.E. (1963) The amino acid sequence of egg white lysozyme. *J. Biol. Chem.* **238**, 2698–2707
2. Jollès, J., Jauregui-Adell, J., Bernier, I., and Jollès, P. (1963) La structure chimique du lysozyme de blanc d'oeuf de poule: etude detailee. *Biochim. Biophys Acta* **78**, 668–689
3. Blake, C.C.F., Koenig, D.F., Mair, G.A., North, A.C.T., Phillips, D.C., and Serma, V.R. (1965) Structure of hen egg white lysozyme. A three-dimensional Fourier synthesis at 2 Å resolution. *Nature* **206**, 757–761
4. Inoue, M., Imada, M., and Tsugita, A. (1970) The amino acid sequence of T4 phage lysozyme. IV. Diluted acid hydrolysis and order of tryptic peptides. *J. Biol. Chem.* **245**, 3479–3484
5. Matthews, B.W. and Remington, S.J. (1974) The three-dimensional structure of the lysozyme from bacteriophage T4. *Proc. Natl. Acad. Sci. USA* **71**, 4178–4182
6. Simpson, R.J. and Morgan, F.J. (1983) Complete amino acid sequence of embden goose (*Anwer anwer*) egg-white lysozyme. *Biochim. Biophys. Acta* **744**, 349–351
7. Grütter, M.G., Weaver, L.H., and Matthews, B.W. (1983) Goose lysozyme structure: an evolutionary link between hen and bacteriophage lysozyme? *Nature* **303**, 828–831
8. Isaacs, N.W., Machin, K.J., and Masakuni, M. (1985) Three-dimensional structure of goose-type lysozyme from the egg white of the Austalian black swan, *Cygnus atratus*. *Aust. J. Biol. Sci.* **38**, 13–22
9. Weaver, L.H., Grütter, M.G., and Matthews, B.W. (1995) The refined structures of goose lysozyme and its complex with a bound trisaccharide show that the "goose-type" lysozymes lack a catalytic aspartate residue. *J. Mol. Biol.* **245**, 54–68
10. Schoentgen, F., Jollès, J., and Jollès, P. (1982) Complete amino acid sequence of ostrich (*Struthio camelus*) egg-white lysozyme, a goose type lysozyme. *Eur. J. Biochem.* **123**, 489–497
11. Richard, J.S., Geoffrey, S.B., Donna, S.D., and Francis, J.M. (1980) Complete amino acid sequence of the goose-type lysozyme from the egg white of the black swan. *Biochemistry* **19**, 1814–1819
12. Thammasirirak, S., Torikata, T., Takami, K., Murata, K., and Araki, T. (2002) The primary structure of Cassowary (*Casuarius casusrius*) goose type lysozyme. *Biosci. Biotechnol. Biochem.* **66**, 147–156
13. Pooart, J., Torikata, T., and Araki, T. (2004) The primary structure of a novel goose-type lysozyme from Rhea egg white. *Biosci. Biotechnol. Biochem.* **68**, 159–169
14. Nakano, T. and Graf, T. (1991) Goose type lysozyme gene of the chicken: Sequence genomic organization and expression reveals major differences to chicken-type lysozyme gene. *Biochim. Biophys Acta* **1090**, 273–276
15. Hikima, J., Minagawa, S., Hirono, I., and Aoli, T. (2001) Molecular cloning, expression and evolution of the Japanese flounder goose-type lysozyme gene, and the lytic activity of its recombinant protein. *Biochim. Biophys Acta* **1520**, 35–44
16. Yin, S., Weng, S., Deng, W., and He, J. (2002) Molecular cloning, expression on the goose-type lysozyme cDNA from orange-spotted grouper (*Epinephelus coioides*), and the lytic activity of its recombinant protein. *Aquaculture Asia* **3**, 21–22
17. Arnheim, N., Inouye, M., Law, L., and Laudin, A. (1973) Chemical studies on the enzymatic specificity of goose egg white lysozyme. *J. Biol. Chem.* **248**, 233–236
18. Honda, Y. and Fukamizo, T. (1998) Substrate binding subsites of chitinase from barley seeds and lysozyme from goose egg white. *Biochim. Biophys Acta* **1388**, 53–65
19. Phillips, D.C. (1966) The three-dimensional structure of an enzyme molecule. *Sci. Am.* **215**, 78–90
20. Imoto, T., Johnson, L.N., North, A.C.T., Phillips, D.C., and Rupley, J.A. (1972) Lysozyme in *Enzymes* (Boyer, P.D., ed.) Vol. 7, 3rd ed., pp. 665–868, Academic Press, New York
21. Strynadka, N.C. and James, M.N.G. (1991) Lysozyme revisited: crystallographic evidence for distortion of an *N*-acetylmuramic acid residue bound in site D. *J. Mol. Biol.* **220**, 401–424
22. Hashimoto, Y., Yamada, K., Motoshima, H., Omura, T., Yamada, H., Yasukochi, T., Miki, T., Ueda, T., and Imoto, T. (1996) A mutation study of catalytic residue Asp52 in hen egg white lysozyme. *J. Biochem.* **119**, 145–150
23. Vocadlo, D.J., Davies, G.J., Laine, R., and Withers, S.G. (2001) Catalysis by hen egg-white lysozyme proceeds via a covalent intermediate. *Nature* **412**, 835–838
24. Kuroki, R., Weaver, L.H., and Matthews, B.W. (1993) A covalent enzyme-substrate intermediate with saccharide distortion in a mutant T4 lysozyme. *Science* **262**, 2030–2033
25. Kuroki, R., Weaver, L.H., and Matthews, B.W. (1995) Structure-based design of a lysozyme with altered catalytic activity. *Nat. Struct. Biol.* **2**, 1007–1011
26. Kuroki, R., Yamada, H., Moriyama, T., and Imoto, T. (1986) Chemical mutations of the catalytic carboxyl groups in lysozyme to the corresponding amides. *J. Biol. Chem.* **261**, 13571–13574
27. Malcolm, B.A., Rosenberg, S., Corey, M.J., Allen, J.S., Baetselier, A.D., and Kirsch, J.F. (1989) Site-directed mutagenesis of the catalytic residues Asp-52 and Glu-35 of chicken egg white lysozyme. *Proc. Natl. Acad. Sci. USA* **86**, 133–137
28. Anand, N.N., Stephen, E.R., and Narang, S.A. (1988) Mutation of active site residues in synthetic T4-lysozyme gene and their

effect on lytic activity. *Biochem. Biophys. Res. Commun.* **153**, 862–868
29. Rennell, D., Bouvier, S.E., Hardy, L.W., and Poteete, A.R. (1991) Systematic mutation of bacteriophage T4 lysozyme. *J. Mol. Biol.* **222**, 67–87
30. Kawamura, S., Fukamizo, T., Araki, T., and Torikata, T. (2003) Expression of a synthetic gene coding for ostrich egg-white lysozyme in *Pichia pastoris* and its enzymatic activity. *J. Biochem.* **133**, 123–131
31. Rupley, J.A. (1964) The hydrolysis of chitin by concentrated hydrochloric acid, and the preparation of low-molecular weight substrates for lysozyme. *Biochim. Biophys Acta* **83**, 245–255
32. Yamada, H., Fukumura, T., Ito, Y., and Imoto, T. (1985) Chitin-coated celite as an affinity adsorbent for high-performance liquid chromatography. *Anal. Biochem.* **146**, 71–74
33. Sarkar, G. and Sommer, S.S. (1990) The "megaprimer" method of site-directed mutagenesis. *Biotechniques* **8**, 404–407
34. Becktel, W.J. and Schellman, J.A. (1987) Protein stability curves. *Biopolymers* **26**, 1859–1877
35. Pace, C.N. (1990) Measuring and increasing in protein stability. *Trends Biotechnol.* **8**, 93–98
36. Hashimoto, Y., Koyabu, N., and Imoto, T. (1998) Effects of signal sequences on the secretion of hen lysozyme by yeast: construction of four secretion cassette vectors. *Protein Eng.* **11**, 75–77
37. Hashimoto, Y., Koyabu, N., and Imoto, T. (1998) Optimization of cultivation time for recombinant protein expression from yeast using αF signal sequence. *Protein Pept. Lett.* **5**, 15–18
38. Koganesawa, N., Aizawa, T., Masaki, K., Matsuura, A., Nimori, T., Bando, H., Kawano, K., and Nitta, K. (2001) Construction of an expression system of insect lysozyme lacking thermal stability: the effect of secretion of signal sequence on level of expression in the Pichia pastoris expression system. *Protein Eng.* **14**, 705–710
39. Mine, S., Ueda, T., Hashimoto, Y., and Imoto, T. (1997) Improvement of the folding yield and solubility of hen egg-white lysozyme by altering the Met residue attached to its N-terminus to Ser. *Protein Eng.* **10**, 1333–1338
40. Takeshita, K., Hashimoto, Y., Tsujihata, Y., So, T., Ueda, T., and Imoto, T. (2004) Determination of the complete cDNA sequence, construction of expression systems, and elucidation of fibrinolytic activity for Tapes japonica lysozyme. *Protein Expr. Purif.* **36**, 254–262
41. Chipman, D.M., Grisaro, V., and Sharon, N. (1967) The binding of oligosaccharides containing N-acetylglucosamine and N-acetylmuramic acid to lysozyme. The specificity of binding subsites. *J. Biol. Chem.* **242**, 4388–4394
42. Fukamizo, T., Amano, S., Yamaguchi, K., Yoshikawa, T., Katsumi, T., Saito, J., Suzuki, M., Miki, K., Nagata, Y., and Ando, A. (2005) *Bacillus circulans* MH-K1 Chitosanase: amino acid residues responsible for substrate binding. *J. Biochem.* **138**, 563–569
43. Ikeda, K. and Hamaguchi, K. (1969) The binding of N-acetylglucosamine to lysozyme. Studies on circular dichroism. *J. Biochem.* **66**, 513–520
44. Fukamizo, T., Ikeda, Y., Ohkawa, T., and Goto, S. (1992) 1H-NMR study on the chitotrisaccharide binding to hen egg white lysozyme. *Eur. J. Biochem.* **210**, 351–357
45. Inoue, M., Yamada, H., Yasukochi, Y., Kuroki, R., Miki, T., Horiuchi, T., and Imoto, T. (1992) Multiple role of hydrophobicity of tryptophan-108 in chicken lysozyme: structural stability, saccharide binding ability, and abnormal pK_a of glutamic acid-35. *Biochemistry* **31**, 5545–5553
46. Inoue, M., Yamada, H., Hashimoto, Y., Yasukochi, T., Hamaguchi, K., Miki, T., Horiuchi, T., and Imoto, T. (1992) Stabilization of a protein by removal of unfavorable abnormal pK_a: substitution of undissociable residue for glutamic acid-35 in chicken lysozyme. *Biochemistry* **31**, 8816–8821
47. Inoue, M., Yamada, H., Yasukochi, T., Miki, T., Horiuchi, T., and Imoto, T. (1992) Left-sidede substrate binding of lysozyme: evidence for the involvement of asparagine-46 in the initial binding of substrate to chicken lysozyme. *Biochemistry* **31**, 10322–10330
48. Ito, Y., Kuroki, R., Ogata, Y., Hashimoto, Y., Sugimura, K., and Imoto, T. (1999) Analysis of a catalytic pathway via a covalent adduct of D52E hen egg white lysozyme by further mutation. *Protein Eng.* **12**, 327–331
49. Monzingo, A.F., Marcotte, E.M., Hart, P.J., and Robertus, J.D. (1996) Chitinases, chitosanases, and lysozymes can be divided into prokaryotic and eukaryotic families sharing a conserved core. *Nature Struct. Biol.* **3**, 133–140
50. Hollis, T., Honda, Y., Fukamizo, T., Marcotte, E., Day, P.J., and Robertus, J.D. (1997) Kinetic analysis of barley chitinase. *Arch. Biochem. Biophys.* **344**, 335–342
51. Brameld, K.A. and Goddard, III, W.A. (1998) The role of enzyme distortion in the single displacement mechanism of family 19 chitinases. *Proc. Natl. Acad. Sci. USA* **95**, 4276–4281
52. Fukamizo, T., Honda, Y., Goto, S., Boucher, I., and Brzezinski, R. (1995) Reaction mechanism of chitosanase from *Streptomyces* sp. N174. *Biochem. J.* **311**, 377–383
53. McCarter, J.D. and Withers, S.G. (1994) Mechanisms of enzymatic glycoside hydrolysis. *Curr. Opin. Struct. Biol.* **4**, 885–892
54. Andersen, M.D., Jensen, A., Robertus, J.D., Leah, R., and Skriver, K. (1997) Heterologous expression and characterization of wild-type and mutant forms of a 26 kDa endochitinase from barley (*Hordeum vulgare* L.). *Biochem. J.* (1997) **322**, 815–822
55. Boucher, I., Fukamizo, T., Honda, Y., Willick, G.E., Neugebauer, W.A., and Brzezinski, R. (1995) Site-directed mutagenesis of evolutionary conserved carboxylic amino acids in the chitosanase from *Streptomyces* sp. N174 reveals two residues essential for catalysis. *J. Biol. Chem.* **270**, 31077–31082
56. Liu, L. and Santi, D.V. (1993) Asparagine 229 in thymidylate synthase contributes to, but is not essential for, catalysis. *Proc. Natl. Acad. Sci. USA* **90**, 8604–8608
57. Liu, L. and Santi, D.V. (1993) Exclusion of 2′-deoxycytidine 5′-monophosphate by asparagines 229 of thymidylate synthase. *Biochemistry* **32**, 9263–9267
58. Schimmel, P. (1993) Functional analysis suggests unexpected role for conserved active-site residue in enzyme of known structure. *Proc. Natl. Acad. Sci. USA* **90**, 9235–9236
59. Shoichet, B.K., Baase, W.A., Kuroki, R., and Matthews, B.W. (1995) A relationship between protein stability and protein function. *Proc. Natl. Acad. Sci. USA* **92**, 452–456
60. Hibler, D.W., Stolowich, N.J., Reynolds, M.A., and Gerlt, J.A. (1987) Site-directed mutants of staphylococcal nuclease. Detection and localization by 1H NMR spectroscopy of conformational changes accompanying substitutions for glutamic acid-43. *Biochemistry* **26**, 6278–6286
61. Zhi, W., Srere, P.A., and Evans, C.T. (1991) Conformational stability of pig citrate synthase and some active-site mutants. *Biochemistry* **30**, 9281–9286
62. Meiering, E.M., Serrano, L., and Fersht, A.R. (1992) Effect of active site residues in barnase on activity and stability. *J. Mol. Biol.* **225**, 585–589